PHYSICAL REVIEW B VOLUME 40, NUMBER 1 1 JULY 1989

Dipolar NMR line shape in a crystal with nonequivalent sites

M. Engelsberg, Ricardo E. de Souza, and Paulo H. Valadares Pereira
Departamento de Física, Universidade Federal de Pernambuco, 50.739 Recife, Pernambuco, Brazil

(Received 19 October 1988)

We have performed ^{19}F pulsed NMR measurements in a single crystal of the cubic perovskite $KZnF_3$. For an orientation of the magnetic field along [110], a distinctive feature of the line shape not previously identified becomes apparent in the derivative of the absorption spectrum. A pattern of four resolved peaks which constitute a dipolar signature of the two types of nonequivalent ^{19}F sites present for this orientation was observed in the absorption-derivative spectrum. For this peculiar line shape a closed expression was derived using continued-fraction approximants. The model line shape was in good agreement with the data without introducing adjustable parameters.

I. INTRODUCTION

The calculation of the spin correlation function which determines the dipolar NMR line shape in a rigid lattice of spin-$\frac{1}{2}$ nuclei has become a classic problem which attracted considerable interest for many years. To a large extent much of the effort was motivated by the existence of an almost ideal system which permitted rather accurate tests of the various types of approximations usually employed in the calculations. Such a system is CaF_2 where the 100% abundant spin-$\frac{1}{2}$ ^{19}F nuclei form a simple cubic lattice of spins interacting via magnetic dipole-dipole interactions with essentially no other magnetic moments present. Since the pioneering work of Lowe and Norberg[1] many different approaches[2,3] have been proposed which have permitted an accurate description of the high-temperature spin auto-correlation function for increasingly longer times.[4]

In CaF_2 each fluorine spin is surrounded by six nearest neighbors and twelve next-nearest neighbors and the ^{19}F NMR absorption spectrum obtained by Fourier transforming the free-induction decay (FID) is quite featureless. The characteristic structure that can be sometimes observed, for example, when the dominant dipolar interactions arise from a small cluster of spins, is absent in CaF_2. This fine structure of magnetic dipolar origin often constitutes an important signature which enables one to monitor a variety of physical, chemical, and even biological processes. A well-known example is the famous Pake[5] doublet.

It is generally accepted that when each spin in a crystal interacts with a large number of neighbors via magnetic dipole-dipole interactions, as in CaF_2 for example, no distinctive signature of dipolar origin in the NMR spectrum can be expected. Although this statement is in general correct, some interesting exceptions are possible when the periodic arrangement of spins in the crystal does not constitute a Bravais lattice. In this case one can find situations where each spin interacts with many neighbors but these neighbors form, for example, two groups of nonequivalent spins with relatively small mutual coupling. If for some orientation of the magnetic field, not only the mutual coupling becomes small but also the internal dipolar couplings within one group attain strengths which are largely different from the coupling strengths within the other group, a quite distinctive line shape can be obtained. This line shape will display a pattern resembling the superposition of two unshifted resonances involving a narrow and a broad component and may lead to the appearance of well-resolved peaks in the *derivative* of the NMR absorption spectrum.

The situation described above can be realized in practice to a good approximation in many crystals with the perovskite structure. We report the result of our measurements of ^{19}F FID signals in a single crystal of the cubic perovskite $KZnF_3$. For an orientation of the external magnetic field parallel to a [110] direction, the derivative of the line shape exhibits very distinctive peaks which constitute a dipolar signature of the two types of nonequivalent ^{19}F spins existing for this particular orientation. The presence of nonequivalent ^{19}F spins in this crystal structure can of course be easily detected by NMR if one totally substitutes the Zn atoms by a magnetic species like Mn or Ni. In this case, up to three different paramagnetically shifted resonances, corresponding to three nonequivalent ^{19}F spins in the unit cell, can be observed for some orientations of the crystal with respect to the external magnetic field.[6,7]

Given the importance of crystals with the perovskite structure in many physical phenomena and the characteristic signature in the derivative of the absorption spectrum, a closed expression for the spin correlation function describing this peculiar line shape was derived. Continued-fraction approximants to the spin autocorrelation function incorporating an arbitrary number of moments have been reported[8] and shown to accurately describe various types of NMR line shapes when a sufficient number of moments are computed. In the present case we employed continued-fraction approximants involving the second and fourth moments. Although only these two moments were included, the postulated two-component asymptotic line shape and the superposition of their individual continued-fraction approximants was sufficient to yield a good fit with no adjustable parameters.

II. DIPOLAR NMR LINE SHAPE IN KZnF$_3$

KZnF$_3$ is a member of the perovskite family of crystals which includes a large number of systems of considerable physical interest. This particular crystal is especially suitable for dipolar NMR line-shape studies because zinc is nonmagnetic and possesses no nuclear magnetic moment whereas ^{39}K nuclei possess a very small magnetic moment compared to fluorine nuclei. Thus the magnetic dipole-dipole interaction among ^{19}F spins is by far the predominant interaction.

The KZnF$_3$ unit cell (Fig. 1) shows the arrangement of ^{19}F nuclei which occupy the centers of the cube faces. This arrangement, unlike the one in CaF$_2$, does not constitute a Bravais lattice by itself. Instead it can be viewed as originating from a simple cubic Bravais lattice of lattice constant[9] $a=4.040$ Å, by assigning to each site a basis of three fluorine atoms at coordinates $A(\frac{1}{2},0,0)$, $\overline{A}(0,\frac{1}{2},0)$, and $B(0,0,\frac{1}{2})$ measured from the center of the unit cell (Fig. 1). Although each fluorine is surrounded by eight nearest neighbors, a larger number than in CaF$_2$, and six next-nearest neighbors, a quite distinctive dipolar signature in the derivative of the ^{19}F NMR absorption spectrum of KZnF$_3$ can be observed for some orientations of the crystal with respect to the external magnetic field $\mathbf{B}_0$.

When $\mathbf{B}_0$ is along a [110] crystal direction the magnetic dipole-dipole interactions of spins A and $\overline{A}$ (Fig. 1) with other fluorine nuclei are identical and these two types of spins can be considered as equivalent. Fluorine spins of B type, on the other hand, have different dipolar interactions with some neighboring spins and must be considered as being nonequivalent to the $A\overline{A}$ group.

The quantity of interest in a pulsed NMR experiment, where the system of spins is prepared by a $\pi/2$ pulse, is the spin autocorrelation function[10]

$$f(t)=\mathrm{Tr}(e^{-iH_d t/\hbar}I_x e^{iH_d t/\hbar}I_x)/\mathrm{Tr}(I_x^2) \tag{1}$$

describing the free-induction decay signal. In Eq. (1) H_d represents the high-field secular dipolar Hamiltonian and I_x denotes the total spin component transverse to the external magnetic field $\mathbf{B}_0$ assumed to be aligned along the z axis.

In KZnF$_3$ with $\mathbf{B}_0 \| [110]$ one can write

$$H_d=H_A+H_B+H_{AB}\ , \tag{2}$$

where H_A represents the dipolar interaction among the N_A fluorine nuclei of type $A(\overline{A})$ (Fig. 1), H_B denotes the dipolar coupling among the $N_B=N_A/2$ fluorine nuclei of type B and the mutual coupling between spins of type $A(\overline{A})$, and type B is represented by H_{AB}. The nonequivalence between the two groups of spins does not exclude the possibility that the coupling term H_{AB} in Eq. (2) may become negligible compared to the sum of the other two terms for some orientation of the crystal with respect to $\mathbf{B}_0$. In that case, since $[H_A,H_B]=0$, the total Hamiltonian $H_d \approx H_A+H_B$ reduces to a sum of two commuting terms and the autocorrelation function of Eq. (1) can be readily shown to separate into a sum of two independent terms,

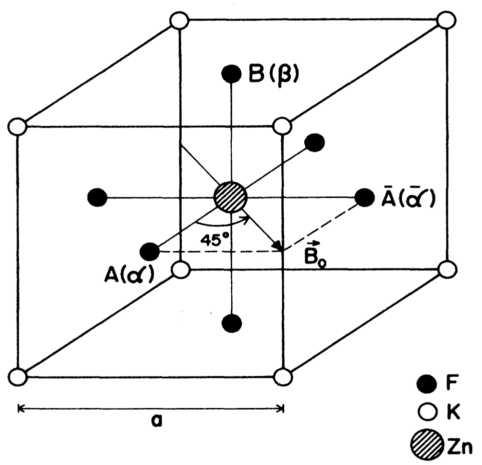

FIG. 1. Unit cell of the cubic perovskite structure showing the atomic positions in KZnF$_3$.

$$f(t)\approx\left[\frac{N_A}{N_A+N_B}\right]\frac{\mathrm{Tr}_A(e^{-iH_A t/\hbar}I_{XA}e^{iH_A t/\hbar}I_{XA})}{\mathrm{Tr}_A(I_{XA}^2)} + \left[\frac{N_B}{N_A+N_B}\right]\frac{\mathrm{Tr}_B(e^{-iH_B t/\hbar}I_{XB}e^{iH_B t/\hbar}I_{XB})}{\mathrm{Tr}_B(I_{XB}^2)}\ . \tag{3}$$

Here Tr_A and Tr_B denote traces with respect to a basis of A spins and B spins, respectively, I_{XA} and I_{XB} denote total spin components within the two groups of spins, and $I_X=I_{XA}+I_{XB}$.

The approximation of completely neglecting the coupling term H_{AB} in Eq. (3) can be improved in a standard way by introducing a small Gaussian broadening which restores the correct value or the total second moment. Thus the first term in Eq. (3) should be multiplied by $e^{-(1/2)(M_{2AB})t^2}$ and the second term by $e^{-(1/2)(M'_{2AB})t^2}$, where M_{2AB} represents the contribution to the second moment of a central A spin due to interactions with neighboring B spins and M'_{2AB} denotes the contribution to the second moment of a central B spin due to dipolar interactions with neighboring $A(\overline{A})$ spins.

The calculation of the individual autocorrelation functions in Eq. (3) corresponding to spins of type $A(\overline{A})$ and B is still difficult. Among the many approaches that have been proposed to deal with this problem, one that has attracted considerable interest addresses the question of obtaining a spectral function given a finite number of its moments. The maximum entropy method[11,12] has been recently shown[3] to yield very good results in the CaF$_2$ line-shape problem. Another method which is particularly simple to implement is based upon a continued-fraction expansion in the frequency domain. It has been shown[2,8] that a single ansatz concerning the asymptotic behavior of the coefficients in a continued-fraction representation yields useful approximants which incorporate any desired number of known moments.[8] Although several moments are frequently necessary to obtain accurate results for long times,[13] the particular form for the correlation function adopted in Eq. (3) permits a satisfactory description with only two moments.

For the perovskite structure of $KZnF_3$ with $\mathbf{B}_0\|[110]$ we have computed various ^{19}F dipolar sums. The approximant to the first correlation function of Eq. (3) requires the calculation of second- and fourth-order dipolar sums which determine the A-spin contribution to the second and fourth moments of nuclei of type A. These sums were also calculated for B spins and incorporated into the approximant to the second correlation function of Eq. (3). For the sums involving dipolar couplings among spins of types A and B, only second-order terms were employed in the calculation of the broadening parameters M_{2AB} and M'_{2AB}.

Denoting by $\mathbf{r}_{\alpha\beta}$ the vector joining a spin (of type A) at site α with a spin (of type B) at site β and by $\theta_{\alpha\beta}$ the angle between $\mathbf{r}_{\alpha\beta}$ and $\mathbf{B}_0$, the dipolar sums can be expressed in terms of the adimensional quantities:

$$b_{\alpha\beta}=\left[\frac{a}{r_{\alpha\beta}}\right]^3(1-3\cos^2\theta_{\alpha\beta}) \ . \tag{4}$$

The following second-order F^{19} dipolar sums were computed for $\mathbf{B}_0\|[110]$ in $KZnF_3$:

$$\sum_{\alpha'(\bar{\alpha})} b^2_{\alpha,\alpha'}(\bar{\alpha})=S_A^{(2)}, \quad \sum_{\beta} b^2_{\alpha\beta}=S_{AB}^{(2)}, \quad \sum_{\beta'} b^2_{\beta\beta'}=S_B^{(2)} \ . \tag{5}$$

The $S_A^{(2)}$ sum involves a central F^{19} spin of type A and extends over other neighboring spins also of type A or $\bar{A}$. The $S_B^{(2)}$ sum is similar to the previous one but involves spins of B type. The $S_{AB}^{(2)}$ sum, on the other hand, involves a central A-type spin and extends over neighboring spins of type B.

From the numerical values listed in Table I it is apparent that the second-order AB coupling represented by $S_{AB}^{(2)}$ is considerably smaller than the sum of the other two terms $S_A^{(2)}+S_B^{(2)}$ for $\mathbf{B}_0\|[110]$. Moreover the dipolar coupling among $A(\bar{A})$ spins represented by $S_A^{(2)}$ is much larger than the coupling term among B spins represented by $S_B^{(2)}$. Thus the conditions leading to a two-component line shape with its characteristic signature can be realized in $KZnF_3$ for $\mathbf{B}_0\|[110]$. It is worth noticing that the AB coupling term $S_{AB}^{(2)}$ is not small compared to $S_B^{(2)}$ but rather of the same order. Consequently one can expect the correction term $e^{-(1/2)(M'_{2AB})t^2}$ to significantly affect the decay of the B-spin autocorrelation function of Eq. (3). However, since this decay is much slower than the A-spin decay and is weighted in Eq. (3) by the smaller factor $N_B=N_A/2$ (Fig. 1), the effect of the broadening function $e^{-(1/2)(M'_{2AB})t^2}$ only becomes significant in the overall decay at relatively long times.

The total second moment[14] M_2 can now be calculated from the second-order dipolar sums of Eqs. (5):

$$M_2=\frac{3}{4}\left[\frac{\gamma_N^2\hbar}{a^3}\right]^2[\tfrac{2}{3}(S_A^{(2)}+S_{AB}^{(2)})+\tfrac{1}{3}(S_B^{(2)}+2S_{AB}^{(2)})] \ , \tag{6}$$

where $\gamma_N=2.5166\times10^4$ $sec^{-1}gauss^{-1}$ is the gyromagnetic ratio for F^{19} nuclei. For $KZnF_3$ with $\mathbf{B}_0\|[110]$ one obtains from Eq. (6) and data of Table I $M_2=3.882\times10^9$ sec^{-2}.

Equation (3) and the proposed Gaussian correction suggest that in Eq. (6) we must identify the correction parameters as

$$M_{2AB}=\left[\frac{3}{4}\frac{\hbar\gamma_N^2}{a^3}\right]^2 S_{AB}^{(2)} \quad M'_{2AB}=2M_{2AB} \ . \tag{7}$$

Likewise, the A-spin and B-spin second moments M_{2A} and M_{2B} which enter into the approximants to the two autocorrelation functions of Eq. (3) must be defined from Eq. (6) as

$$M_{2A}=\left[\frac{3}{4}\frac{\hbar\gamma_N^2}{a^3}\right]^2 S_A^{(2)}, \quad M_{2B}=\left[\frac{3}{4}\frac{\hbar\gamma_N^2}{a^3}\right]^2 S_B^{(2)} \ . \tag{8}$$

In addition to the second-order dipolar sums of Eq. (5), the following fourth-order dipolar sums were also computed:

$$S_{A1}^{(4)}=\sum_{\alpha'\neq\alpha''} b^2_{\alpha\alpha'(\bar{\alpha})}b^2_{\alpha\alpha''}(\bar{\alpha}), \quad S_{B1}^{(4)}=\sum_{\beta'\neq\beta''} b^2_{\beta\beta'}b^2_{\beta\beta''} \ , \tag{9a}$$

$$S_{A2}^{(4)}=\sum_{\alpha'\neq\alpha''} b^2_{\alpha'\alpha''}(b_{\alpha\alpha'(\bar{\alpha})}-b_{\alpha\alpha''(\bar{\alpha})})^2 \ ,$$

$$S_{B2}^{(4)}=\sum_{\beta'\neq\beta''} b^2_{\beta'\beta''}(b_{\beta\beta'}-b_{\beta\beta''})^2 \ , \tag{9b}$$

$$S_{A3}^{(4)}=\sum_{\alpha'} b^4_{\alpha\alpha'}(\bar{\alpha}), \quad S_{B3}^{(4)}=\sum_{\beta'} b^4_{\beta\beta'} \ . \tag{9c}$$

The numerical values of these parameters for $\mathbf{B}_0\|[110]$ in the cubic perovskite structure are listed in Table I.

From the fourth-order dipolar sums of Eqs. (9), the individual A-spin and B-spin fourth moments that together with Eqs. (8) completely specify the approximants to the two autorcorrelation functions of Eq. (3) can be calculated. These two fourth moment contributions are given by[14,15]

TABLE I. Dipolar sums for ^{19}F in the cubic perovskite structure of $KZnF_3$.

$S_A^{(2)}$	$S_B^{(2)}$	$S_{AB}^{(2)}$	τ_{1A} (sec)	$S_{A1}^{(4)}$	$S_{A2}^{(4)}$	$S_{A3}^{(4)}$	M_{4A} (sec^{-4})	τ_{2A} (sec)
87.406	5.062	5.494	1.408×10^{-5}	0.546×10^4	1.248×10^4	0.2115×10^4	4.771×10^{19}	1.609×10^{-5}
M_{2A} (sec^{-2})	M_{2B} (sec^{-2})	$2M_{2AB}=M'_{2AB}$ (sec^{-2})	τ_{1B} (sec)	$S_{B1}^{(4)}$	$S_{B2}^{(4)}$	$S_{B3}^{(4)}$	M_{4B} (sec^{-4})	τ_{2B} (sec)
5.042×10^9	0.292×10^9	0.317×10^9	5.852×10^{-5}	22.833	36.845	2.796	1.964×10^{17}	4.490×10^{-5}

$$M_{4A}=\left[\frac{3}{4}\frac{\hbar\gamma_N^2}{a^3}\right]^4(3S_{A1}^{(4)}-\tfrac{1}{3}S_{A2}^{(4)}+S_{A3}^{(4)})\ , \tag{10a}$$

$$M_{4B}=\left[\frac{3}{4}\frac{\hbar\gamma_N^2}{a^3}\right]^4(3S_{B1}^{(4)}-\tfrac{1}{3}S_{B2}^{(4)}+S_{B3}^{(4)})\ . \tag{10b}$$

The model line shape which is expected to describe the behavior of the F^{19} resonance in $KZnF_3$ for $\mathbf{B}_0\|[110]$ can now be given. Instead of the four moments M_{2A}, M_{2B}, M_{4A}, and M_{4B} of Eqs. (8) and Eq. (10), some combinations of these four quantities must be constructed in order to specify the continued-fraction approximants. The new parameters are defined as follows:[7]

$$\tau_{1A}=(M_{2A})^{-1/2},\quad \tau_{1B}=(M_{2B})^{-1/2}\ , \tag{11a}$$

$$\tau_{2A}=\tau_{1A}/(M_{4A}\tau_A^4-1),\quad \tau_{2B}=\tau_{1B}/(M_{4B}\tau_{1B}^4-1)\ . \tag{11b}$$

A closed expression for the continued-fraction approximant to the sought spin correlation function can be written. From Eqs. (A1) of Ref. 8 and Eq. (2) one obtains

$$\begin{aligned} f(t)=&\tfrac{2}{3}e^{-(1/2)(M_{2AB})t^2}\int_{-\Omega_{CA}}^{\Omega_{CA}} g_A(\Omega)\cos\Omega t\,d\Omega\\ &+\tfrac{1}{3}e^{-(1/2)(M'_{2AB})t^2}\int_{-\Omega_{CB}}^{\Omega_{CB}} g_B(\Omega)\cos\Omega t\,d\Omega\ , \end{aligned} \tag{12}$$

where $g_A(\Omega)$ and $g_B(\Omega)$ are given by

$$g_A(\Omega)=\frac{2}{\pi}\frac{(\tau_{1A}\tau_{2A})^{1/2}}{\tau_{2A}/\tau_{1A}}\left[\frac{(1-\Omega^2\tau_{1A}\tau_{2A}/4)^{1/2}}{1+\Omega^2(\tau_{1A}^3/\tau_{2A}-\tau_{1A}^2)}\right]\ , \tag{13a}$$

$$|\Omega|<\Omega_{CA}=2/(\tau_{1A}\tau_{2A})^{1/2}\ , \tag{13b}$$

$$g_B(\Omega)=\frac{2}{\pi}\frac{(\tau_{1B}\tau_{2B})^{1/2}}{\tau_{2B}/\tau_{1B}}\left[\frac{(1-\Omega^2\tau_{1B}\tau_{2B}/4)^{1/2}}{1+\Omega^2(\tau_{1B}^3/\tau_{2B}-\tau_{1B}^2)}\right]\ , \tag{13c}$$

$$|\Omega|<\Omega_{CB}=2/(\tau_{1B}\tau_{2B})^{1/2}\ . \tag{13d}$$

III. EXPERIMENTAL RESULTS AND DISCUSSION

Using a conventional pulsed NMR spectrometer operating at a frequency of 60 MHz we have measured F^{19} FID signals in $KZnF_3$. A single crystal in the form of a cylinder with its axis coincident with a [100] direction and positioned perpendicularly to the external magnetic field $\mathbf{B}_0$ was rotated about [100] and data were recorded for various angles. For $\mathbf{B}_0\|[110]$ the FID develops a characteristic "hump" with its maximum close to 50 μsec (Fig. 2).

The data shown in Fig. 2 were obtained at 77.8 K and were corrected for the effect of a finite 210-KHz bandwidth of the receiver system. The small correction consisted of a shift[16] of 1.5 μsec of the origin of the FID from the center of the 1.7-μsec π/2 pulse towards longer times. In the region where the receiver is blocked, the data shown as circles in Fig. 2 correspond to a Gaussian extrapolation.

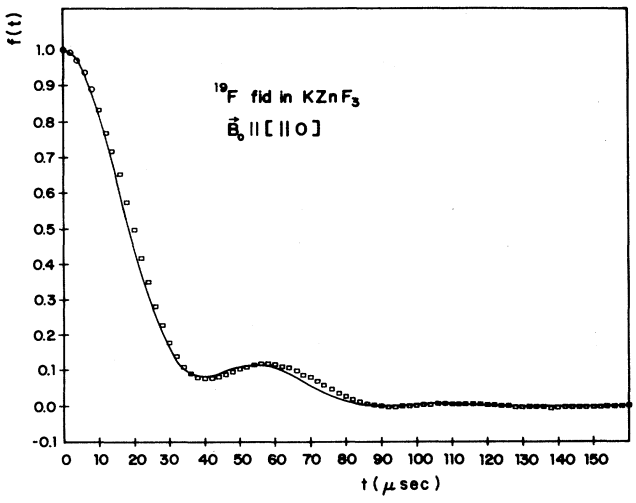

FIG. 2. ^{19}F FID signal in $KZnF_3$ for $\mathbf{B}_0\|[110]$ (□). The solid line is the calculated autocorrelation function obtained from Eqs. (12) and (13) and the computed dipolar lattice sums of Table I.

In the frequency domain the characteristic signature of the two types of nonequivalent ^{19}F spins becomes more striking if one examines the derivative of the NMR line shape. Figure 3 shows the derivative absorption spectrum obtained by a Fourier transformation of the data of Fig. 2 followed by differentiation. The pattern of four peaks observable in Fig. 3 was also present as expected in spectra obtained by the cw method. These four peaks, involving four maxima and two minima, correspond to the six inflection points of a well-resolved two-component line shape consisting of a broad line and a narrower one.

The result of our model calculation obtained from Eqs. (12) and (13) with the computed values of the parameters listed in Table I is also shown in Fig. 3 together with the experimental FID. The agreement is very good without any adjustment in the numerical value of the parameters of Table I. The spectrum obtained by a Fourier transformation and differentiation of the correlation function $f(t)$ of Eqs. (12) and (13) and shown in Fig. 3 clearly

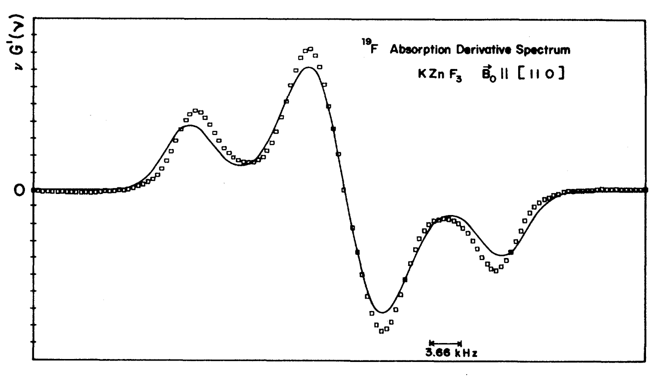

FIG. 3. ^{19}F absorption-derivative spectrum in $KZnF_3$ for $\mathbf{B}_0\|[110]$ (□). The solid line is the calculated derivative of the line shape.

displays the characteristic peaks present in the experimental spectrum and is also in good agreement with the data. Moreover some of the discrepancy between the experimental FID and the calculated correlation function may still be attributed to a slight misalignment of the crystal which we estimated to be less than 3°. In fact the experimental value of the second moment obtained from a Gaussian fit of the initial part of the FID decay signal of Fig. 1 was $M_2(\text{expt})=(3.6\pm0.1)\times10^9\ \text{sec}^{-2}$. Although this value is slightly smaller than the theoretical value $M_2(\text{theory})=3.88\times10^9\ \text{sec}^{-2}$ we preferred to compare the data of Fig. 1 with the calculated correlation function using the theoretical values of all parameters. Small variations of these parameters from the values listed in Table I could actually improve the fit.

In the computation of the lattice sums listed in Table I clusters of radii as large as 40 lattice constants were employed in some cases. Since the estimated increase of the second moment due to interactions with potassium nuclei was less than 1%, the effect was considered negligible and only dipolar interactions among ^{19}F nuclei were considered.

Although a detailed comparison with other line-shape theories has not been attempted in this work we may conclude that the explicit form of the correlation function $f(t)$ of Eqs. (12) and (13) with the parameters of Table I permits a quite accurate description of the dipolar NMR line shape in the perovskite structure for $\mathbf{B}_0\|[110]$. For this orientation, the derivative of the absorption spectrum displays a characteristic pattern composed of four peaks which should be a helpful signature in cases where other interactions in these crystals are present. Such may be the case, for example, when magnetic ions are substitutionally introduced into these crystals to study various properties of randomly diluted magnetic systems or when quadrupole interactions are present.

ACKNOWLEDGMENTS

We wish to thank Afonso H. S. da Costa e Silva for skillful help. We are much indebted to Professor Geraldo A. Barbosa of the Universidade Federal de Minas Gerais for making available a $KZnF_3$ single crystal. This work has been supported by Financiadora de Estudos e Projetos (FINEP), Conselho Nacional de Desenvolvimento Científico e Tecnológico (CNPq), and Coordenação de Aperfeiçoamento de Pessoal do Ensino Superior (CAPES).

---

[1] I. J. Lowe and R. E. Norberg, Phys. Rev. **107**, 46 (1957).

[2] See, for example, M. Engelsberg and I. J. Lowe, Phys. Rev. B **12**, 3547 (1975), and references therein.

[3] See, also, P. A. Fedders and A. E. Carlsson, Phys. Rev. B **32**, 229 (1985).

[4] M. Engelsberg and I. J. Lowe, Phys. Rev. B **10**, 822 (1974).

[5] G. E. Pake, J. Chem. Phys. **16**, 327 (1948).

[6] R. G. Shulman and K. Knox, Phys. Rev. **119**, 94 (1960).

[7] M. Engelsberg, Phys. Rev. B **19**, 5942 (1979).

[8] M. Engelsberg and Nai-Cheng Chao, Phys. Rev. B **12**, 5043 (1975).

[9] R. K. Jeck and J. J. Krebs, Phys. Rev. B **5**, 1677 (1972).

[10] A. Abragam, *Principles of Nuclear Magnetism* (Clarendon, Oxford, England, 1961), Chap. 4.

[11] See E. T. Jaynes, in *Papers on Probability, Statistics and Statistical Physics,* edited by R. D. Rosenkrantz (Reidel, Dordrecht, 1983).

[12] Lawrence R. Mead and N. Papanicolau, J. Math. Phys. **25**, 2404 (1984).

[13] Nai-Cheng Chao and M. Engelsberg, Phys. Rev. B **14**, 271 (1976).

[14] J. H. Van Vleck, Phys. Rev. **74**, 1148 (1948).

[15] G. W. Canters and C. S. Johnson, Jr., J. Magn. Reson. **6**, 1 (1972).

[16] D. E. Barnaal and I. J. Lowe, Rev. Sci. Instrum. **37**, 428 (1966).